

Chapter 3

Dimensional Effects of Transistors and Storage Capacitor on Conventional Pixel Circuit Schematic

3.1 Introduction

Organic light emitting diode (OLED) displays have attracted much attention since the first appearance of the high efficient double-layer OLED device which was reported by Tang and Van Slyke in 1987 [3.1]. Owing to various superior features such as fast response time, wide viewing angle, wide color gamut, high brightness, high contrast ratio, simple structure, and low fabrication cost, OLED displays show great advantages over active matrix liquid crystal displays (AMLCDs) [3.2]-[3.4]. In addition, OLED displays are self-emissive devices, they do not need any backlight and can be very compact and thin with lower power consumption. OLED displays can be driven either by passive matrix (PMOLED) or active matrix (AMOLED) according to its driving scheme. Although PMOLEDs are suitable for small-sized displays application with low fabrication cost, simple structure and easy driving [3.5], they can not be applied to the high resolution and large panel-size displays because high voltage and high current are necessary to achieve average brightness across the panel. This would consume more power and degrade OLED device rapidly accompanying with the poor image quality. Therefore, active matrix driving

method which each pixel can provide a constant current throughout the entire frame is preferred for high image content displays in the future in order to reduce the peak current and associated voltage drop in the row/column lines. The voltages and the peak current levels for active driving display are at least two orders magnitude lower than those for passive driving display under the same brightness condition [3.6].

There are many choices for active matrix devices such as single crystal silicon MOSFETs, amorphous thin film transistors (a-Si:H TFTs), high-temperature polycrystalline silicon TFTs (HTPS TFTs), low-temperature polycrystalline silicon TFTs (LTPS TFTs), organic TFTs (OTFTs), etc [3.7]-[3.8]. Among them, LTPS TFTs fabricated by excimer laser crystallization (ELC) have the greatest potential to be employed as the switching devices and pixel driving elements for backplanes both in active organic light emitting diode (AMOLED) and active matrix liquid crystal display (AMLCD) [3.9]-[3.13] because of the high driving capability, large aperture ratio, superior stability, and high thermal endurance. With these good performances, they are adequate to perform driver circuits and can be integrated on the glass substrate to omit additional connection and reduce the cost of driver IC. For AMOLED, transistors are used for switch and steady current source. At least two transistors and one capacitor are required in each pixel to provide continuous excitation throughout the whole frame period [3.14]. The well-known 2T1C pixel design with simple circuit driving schematic was first proposed in 1975 [3.15]. It has relative high aperture ratio than other circuits. Although this circuit structure suffers from pixel to pixel brightness non-uniformity problem, it is easy to fabricate and can be driven by a simple external driver electronics. As a result, it might be a good solution for some small size application such mobile products.

In this chapter, a systematic study is made on the basic design of active matrix pixel circuit. The operation scheme of the basic design for AMOLED is introduced. N-type TFTs circuits are considered and measured. After that, dimensional effects of transistors and

storage capacitor on the traditional 2T1C pixel circuit schematic are investigated based on various simulation and experimental results. In addition to these pixel component effects, slicing layout method of the driving transistor is also designed and introduced in the testing pixel to analysis its impact on the circuit performance.

3.2 Basic Design for AMOLED

3.2.1 Fundamental Element of Pixel Circuits

The fundamental element of the AMOLED pixel circuits consists of one driving transistor and one organic electroluminescent device (OELD) or so called organic light emitting (OLED) in this thesis. The transparent ITO anode and cathode layer of OLED device form a quasi-insulating organic capacitor which is in parallel with the diode and the equivalent circuits is shown in Fig. 3.1. The capacitance is approximately 25nF/cm [3.6]. Unlike AMLCDs, OLEDs are current driven devices and the emitting brightness is a function of the current density flowing though the OLED device. The measured current density – voltage (J-V) – brightness (B) characteristics of OLED is shown in Fig. 3.2. Therefore, the driving transistor must deliver the steady current through OLED device in correspondence with the necessary control voltage (V_{ctrl}) and the panel gray scale is controlled by the applied current. All the driving methods for AMOLEDs have this basic structure, while many variations of the driving scheme come from how to apply the control voltage (V_{ctrl}) to the gate voltage of the driving transistor.

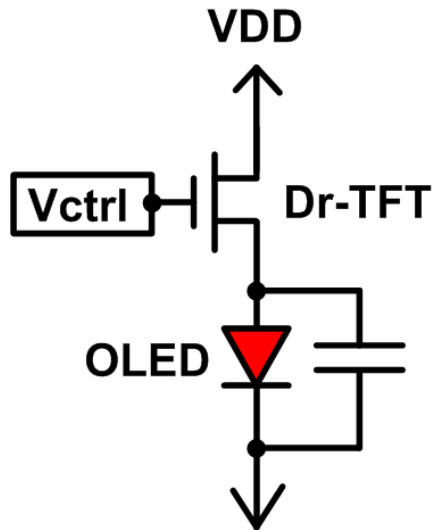


Fig. 3.1. Fundamental element of the AMOLED pixel circuits.

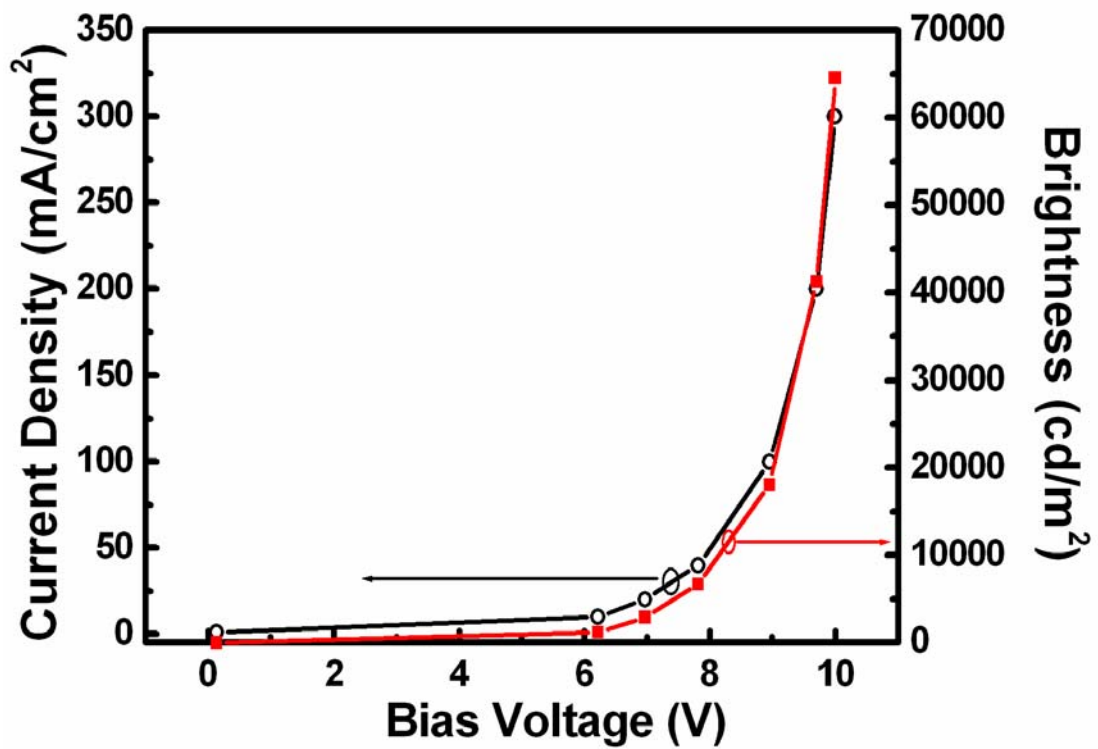


Fig. 3.2. The current density – voltage (J-V) – brightness characteristics of OLED.

3.2.2 Simple Pixel Circuit for AMOLED

For active matrix OLED (AMOLED), it should supply a controlled constant current source to drive OLED device to achieve different grey scales and enable the pixel to illuminate continuously after the addressing period. Fig. 3.2 shows the simple pixel circuit with two transistors and one capacitor. TFT1 is the select transistor, which is employed as a switch. When TFT1 is turned on by the selected scan line, the data signal voltage is transferred to the gate of the driving transistor, TFT2, through TFT1 and stored in the storage capacitor, C_s . Meanwhile, the driving transistor converts the data voltage to data current and then provides a specified current for OLED device. If TFT2 is biased sufficiently to stay in the saturation mode, the drain current will be determined only by the gate to source voltage (V_{gs}) of TFT2 according to the quadratic equation which is shown as follows.

$$I_d = \frac{1}{2} k_2 (V_{gs_T2} - V_{th_T2})^2, \text{ where } k_2 = \mu C_{ox} \frac{W_2}{L_2}.$$

In above equation, μ is the field-effect mobility, C_{ox} is the oxide capacitance per unit area, W_2 and L_2 represent the width and length of the driving TFT, and V_{th_T2} is threshold voltage. Because of the capability of storage capacitor, the brightness of OLED device is maintained until the end of a frame period.

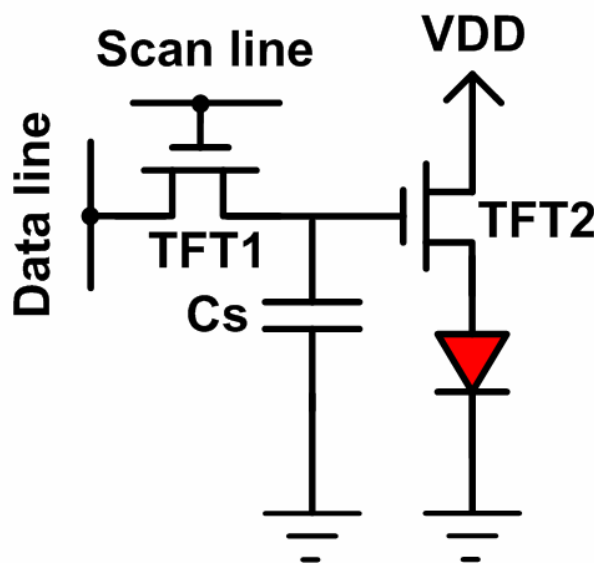


Fig. 3.3. Simple pixel circuit for AMOLED.

3.3 Dimensional Effects of Transistors and Storage

Capacitor

In order to investigate the dimensional effects of transistors and storage capacitor on circuit performance, HSPICE circuit simulator was performed. The diode can be approximated by a SPICE diode with n factor of 39, I_s of 1.241×10^{-5} A/cm² and series resistance of 1×10^{-5} Ω . Fig. 3.4 shows the measured and simulated OLED current versus bias voltage characteristics. In this chapter, the OLED area is assumed to be 60 μm x 220 μm for conventional 2T1C circuit schematic, which corresponds to a 4-inch QVGA specification. Device electrical characteristics of n-type LTPS TFTs were measured by HP4156C measurement system in order to obtain SPICE model. Simulation parameters were extracted from BSIMPro v2 and the simulation model is RPI poly-silicon TFT model (LEVEL 62). Figure 3.5 shows the measured and simulated transfer characteristic of n-channel TFT which shows good fitting results. In the following, four effects on circuit performance are analyzed and studied which include the effect of switching TFT, the effect of driving TFT, the effect of storage capacitor and the effect of transistor slicing layout.

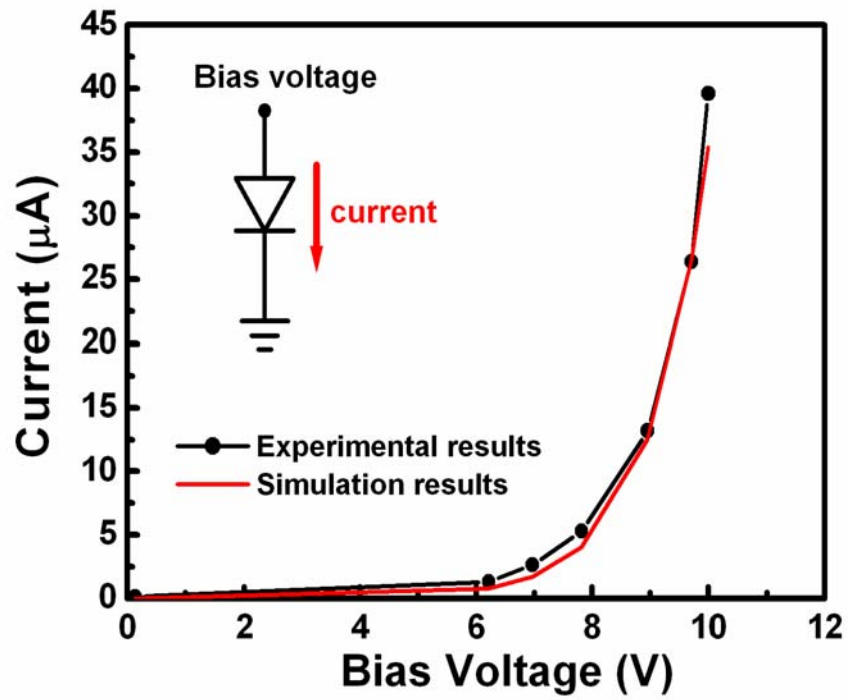


Fig. 3.4. The measured and simulated OLED current versus bias voltage characteristics.

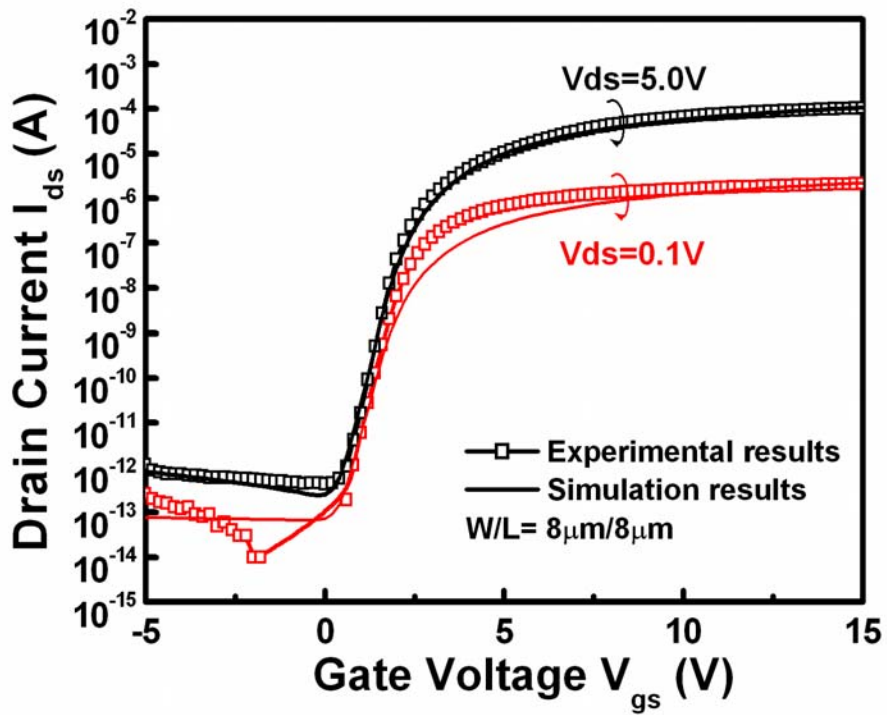


Fig. 3.5. The measured and simulated transfer characteristics of n channel TFTs.

3.3.1 The Effect of Switching TFT

To study the effect of switching TFT on circuit characteristics, three different dimensions are considered, which are $10\ \mu\text{m}/10\ \mu\text{m}$, $10\ \mu\text{m}/20\ \mu\text{m}$, and $20\ \mu\text{m}/10\ \mu\text{m}$. In this case, the power supply line (V_{DD}) is set to be 10V, the scan line (V_{scan}) is a voltage pulse signal with peak value, 10V, and base value, 0V. The dimension of driving TFT is $100\ \mu\text{m}/10\ \mu\text{m}$ and the capacitance of the storage capacitor is assumed to be 0.5pF. The input data voltage (V_{data}) is varied from 1 V to 7V to obtain different output voltages. Fig. 3.6 shows the anode voltage of OLED versus input voltage characteristics. It can be seen obviously that the anode voltage of OLED is proportional to input voltage. Even though the size of switching TFT is varied from $10\ \mu\text{m}/10\ \mu\text{m}$ to $20\ \mu\text{m}/10\ \mu\text{m}$ which is four times larger than the former, the anode voltages are almost the same. As a result, the dimension of switching TFT which is only employed as a switch element for transferring the external applied signal can be decreased to the minimum size according to the design rule in the fabrication process.

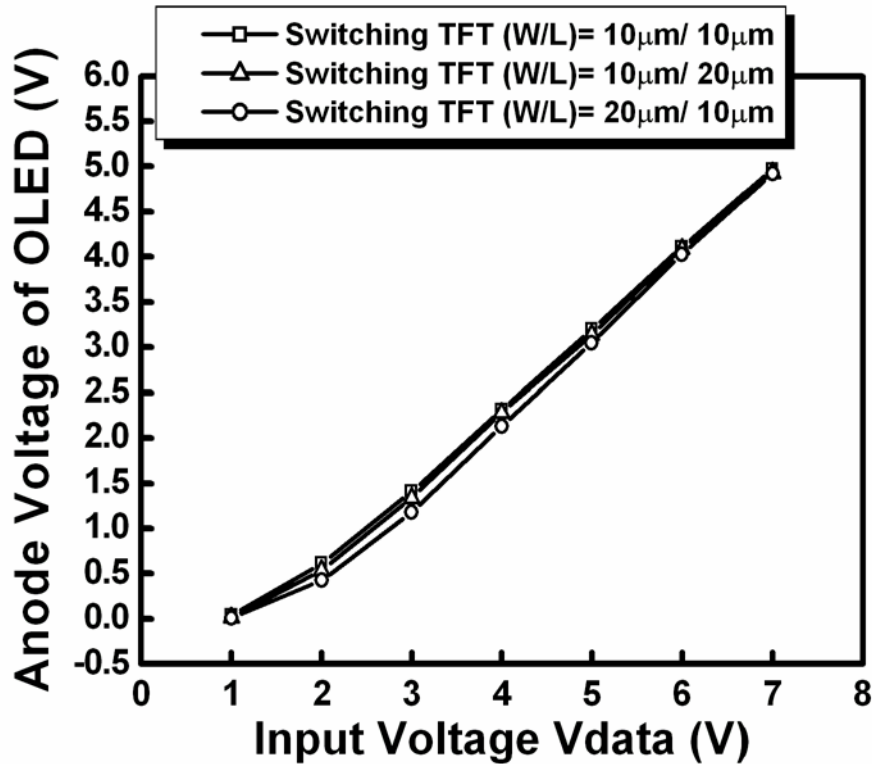


Fig. 3.6. The anode voltage of OLED versus input voltage characteristics with varied dimensions of switching TFTs.

3.3.2 The Effect of Driving TFT

To investigate the role that driving TFT plays in the pixel circuit, dimensional effect of driving TFTs including $10\ \mu\text{m}/10\ \mu\text{m}$, $50\ \mu\text{m}/10\ \mu\text{m}$, $100\ \mu\text{m}/10\ \mu\text{m}$, and $150\ \mu\text{m}/10\ \mu\text{m}$ is considered. The condition of applied voltages is the same as that in section 3.3.2. The size of switching is assumed to be $10\ \mu\text{m}/10\ \mu\text{m}$ and the capacitance of the storage capacitor is set to be 0.5pF . The anode voltage of OLED versus input voltage characteristics is shown in Fig. 3.7. Besides the anode voltage of OLED is a function of input voltage, it is increased with the size of driving TFT. However, the larger driving TFT occupying the substrate will result in the smaller emission area of OLED device. Therefore, the size of driving TFT and the aperture ratio must achieve a balance to obtain the optimum condition for specific display.

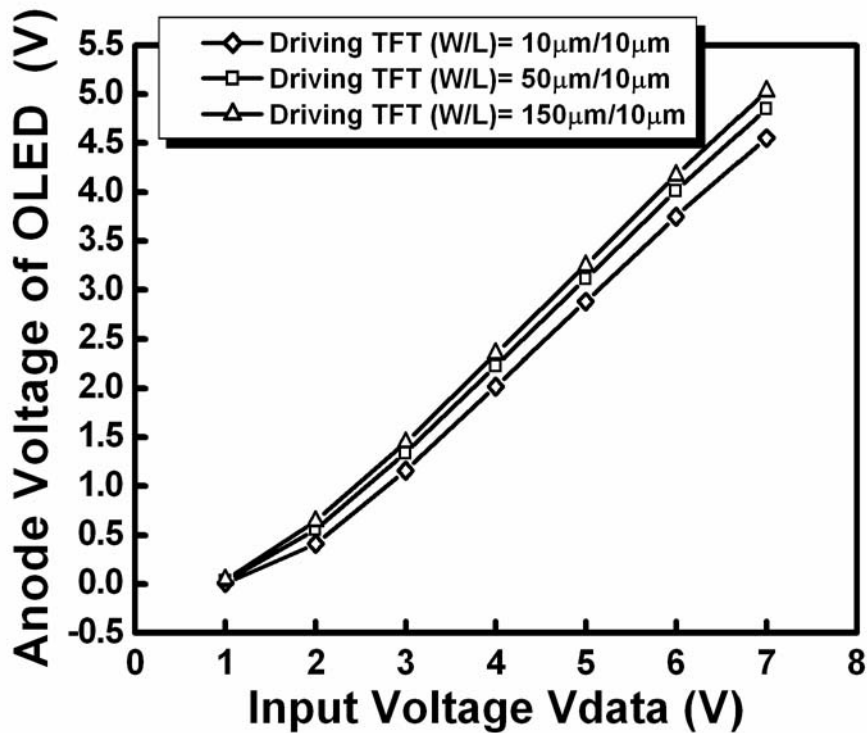


Fig. 3.7. The anode voltage of OLED versus input voltage characteristics when the dimension of driving TFT varies.

3.3.3 The Effect of Storage Capacitor

In order to investigate the dimensional effects of the storage capacitor on pixel circuit performance, two different capacitances of the storage capacitor are considered. One is 0.1pF and the other is 2pF. The conditions of the applied voltages and the dimensions of switching TFT and driving TFT are as follows. $V_{DD} = 10V$. V_{scan} is a voltage pulse signal with peak value, 10V and base value, 0V. V_{data} is set to be 5V. Switching TFT is assumed to be $10 \mu m/10 \mu m$ and driving TFT is $100 \mu m/10 \mu m$. Fig 3.8 shows the stored voltages in the capacitor when $V_{data} = 5V$. It is shown clearly that the magnitude of capacitance will determine the charging time and the holding capability of the capacitor. The larger the storage capacitor is, the better the holding capability to maintain the input data voltage is.

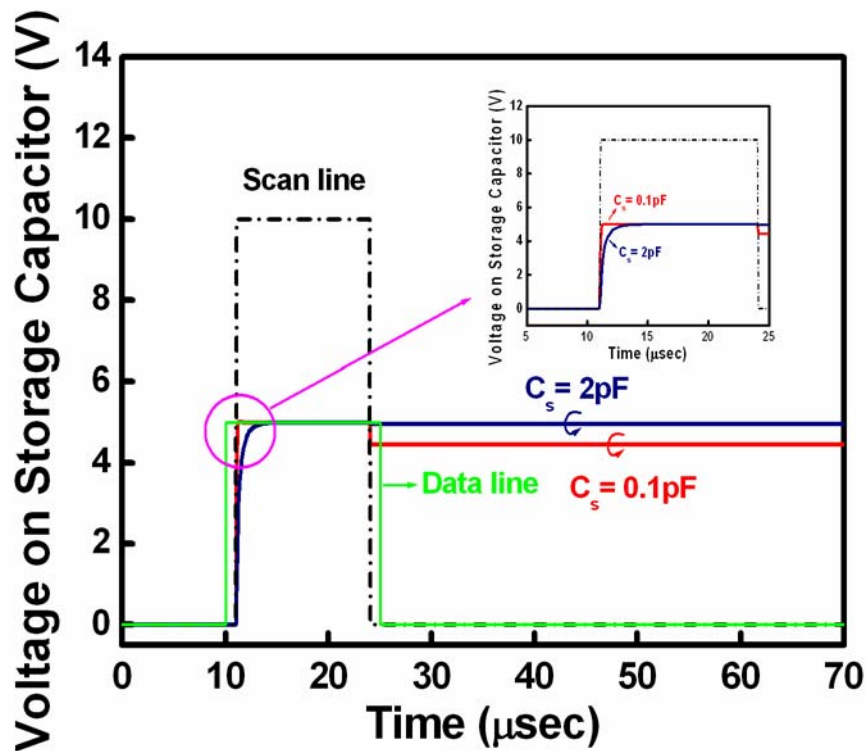


Fig. 3.8. The stored voltages in the capacitors with varied capacitances when $V_{\text{data}} = 5\text{V}$.

3.3.4 The Effect of Transistor Slicing Layout

Transistor slicing layout method means to divide a large transistor into several smaller equal-sized transistors. In this section, the slicing layout is applied on driving TFT. Fig. 3.9 shows the idea of slicing layout method. Conventional layout is a single large TFT and transistor slicing layout means the parallel connection of several smaller equal-sized TFTs. To analyze the effect of slicing layout on the circuit performance, Monte Carlo simulation with an assumption of normal distribution was executed. The mean value and the deviation of the threshold voltage and mobility are 1.55V , $\pm 1\text{V}$, $52.02\text{ cm}^2/\text{V}\cdot\text{s}$, and $\pm 20\text{ cm}^2/\text{V}\cdot\text{s}$, respectively. In this case, ten smaller TFTs with equal $10\text{ }\mu\text{m}/10\text{ }\mu\text{m}$ dimension are used to implement a larger $100\text{ }\mu\text{m}/10\text{ }\mu\text{m}$ driving TFT. Fig. 3.10 shows the anode voltage of OLED versus input voltage characteristics. It is obviously that the OLED anode, that is,

current driving capability of driving TFT with transistor slicing layout is enhanced. Fig. 3.11 shows the non-uniformity of the output current when the input voltage varies from 1V to 6V. Non-uniformity is defined as the difference between the maximum output current and the minimum output current divided by the average output current. It can be seen that the non-uniformity can be reduced effectively from the conventional layout to slicing layout. Because slicing layout can promote the output current for OLED, non-uniformity problem in the circuit can be reduced.

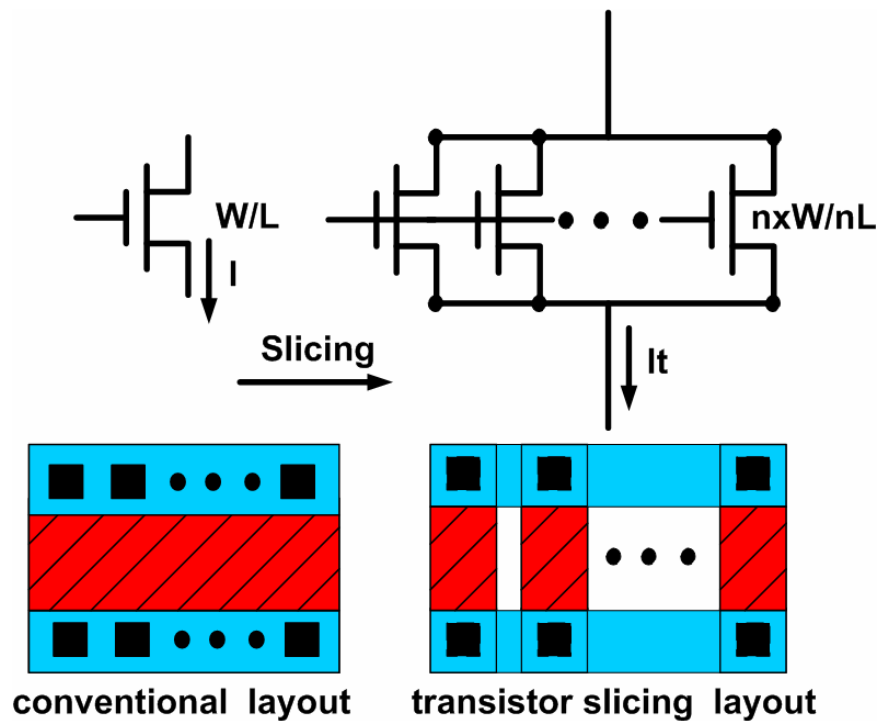


Fig. 3.9. Conventional layout and transistor slicing layout.

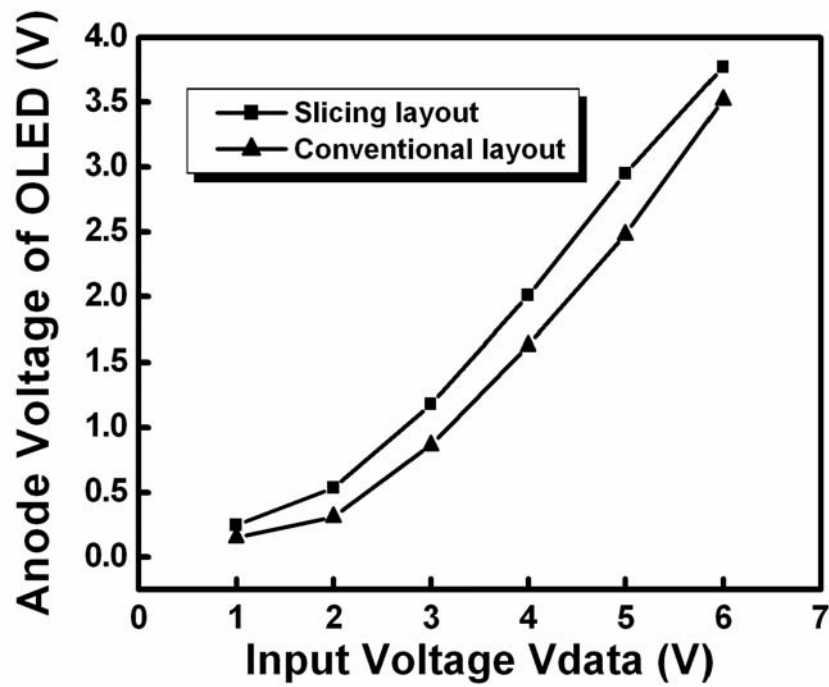


Fig. 3.10. The anode voltage of OLED versus input voltage characteristics with different layout methods.

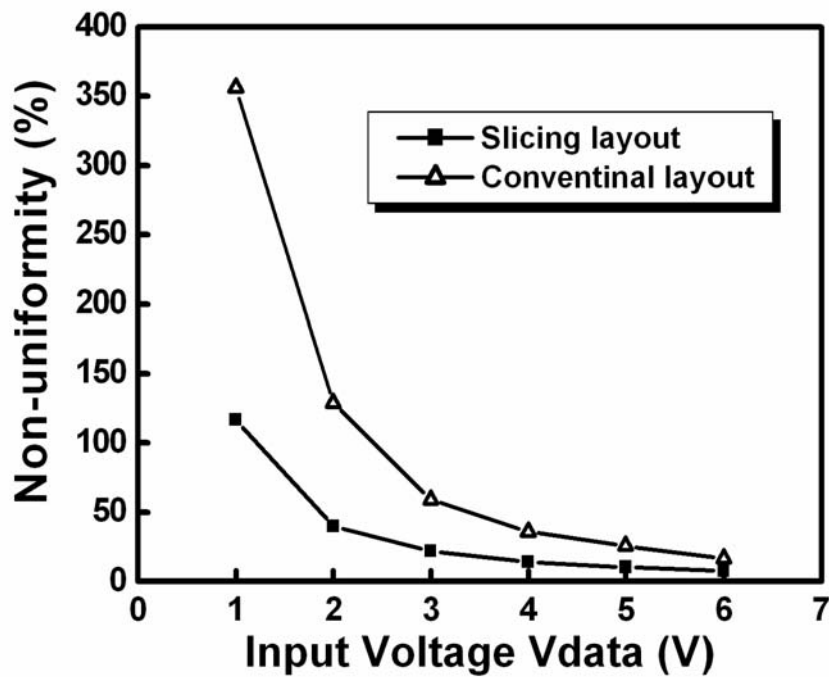


Fig. 3.11. The non-uniformity of the output current when the input voltage varies from 1V to 6V with 10 times Monte Carlo simulation.

3.4 Experimental Results and Discussion

The testing conventional pixel circuits were fabricated by the following sequence of processes. Fig. 3.12 shows the optical micrograph view of the simple pixel circuit design. First, a buffer oxide which consists of a 500 Å SiN_x and a 2500 Å SiO_2 and another 500Å-thick a-Si thin film were deposited on glass substrate by plasma-enhanced chemical vapor deposition (PECVD). Then, the amorphous Si thin film was crystallized by XeCl excimer laser annealing at room temperature in the N_2 gas ambient. After defining the active layer, a 1000Å-thick gate oxide was deposited by PECVD and a 4000Å-thick Cr film was then deposited for gate electrode. The Cr thin film and gate oxide were etched in order to form gate electrodes. Ion implantation was then performed to form source and drain regions. Next, a 4000Å-thick SiN_x was deposited by PECVD as interlayer. The TFT testing pixel circuits were formed after contact-hole formation and 4000Å-thick Cr metallization. In the experiment, the electrical characteristics of an OLED used in the measurement was replaced by a diode-connected TFT and a capacitor whose dimensions are $8 \mu\text{m} / 100 \mu\text{m}$ and 3.3pF in order to represent and match the OLED device.

Fig 3.13 shows the measurement system for conventional 2T1C testing pixel circuits, it includes Agilent 4156C, HP 41501A pulse generator, and Agilent 54622D mixed signal oscilloscope. Agilent 4156C including four probes is the main system. HP 41501A provides two voltage pulses which will apply to the scan line (V_{scan}) and the data line (V_{data}). One additional probe is needed to observe the anode voltage of OLED. Through BNC connection, the output signal voltage (V_{OLED}) can be figured in Agilent 54622D mixed signal oscilloscope. All ground terminals of the employed instruments must connect together. After the measurement system is ready, the output signal voltages were measured. Ten testing pixel circuits have been measured in order to study the dimensional effects of transistors and

storage capacitors on circuit performance.

Fig. 3.14 shows the measured and simulation results of OLED anode voltages versus input voltages when the dimension of switching TFT varies. Fig. 3.15 shows the measured and simulation results of OLED anode voltages versus input voltages when the dimension of driving TFT varies. From the two figures, it is obviously that the simulation results and experimental results show the same tendency of switching TFT and driving TFT impacts on circuit characteristics. The only difference of these two results is the anode voltage of OLED in experimental case is lower than that in the simulation case. The possible reason for this is the large impedance in the real measurement condition that is not considered in the simulation case.

Fig. 3.16 shows the measured results of the stored voltage in the capacitor when $V_{\text{data}} = 5\text{V}$. The period of the input data voltage is set to be $100 \mu\text{sec}$ in order to deal with the large impedance of the measurement system and metal lines. From the experimental results, it is verified that larger capacitor can hold the data voltage effectively, but the charging time is lower than that of smaller capacitor. Therefore, the choice of the capacitance in the pixel is dependent on the demand for specific product specification. Fig. 3.17 shows the simulated and measured results of OLED anode voltage with conventional layout and slicing layout. The anode voltage of OLED can be raised above 30% at $V_{\text{data}} = 3\text{V}$. Fig. 3.18 shows the simulated and measured results of non-uniformity with conventional layout and slicing layout. From the cross-section of driving TFT with slicing layout as shown in Fig. 3.19, it can be seen that the gate electrode across the channel may induce side-channels in both sides of the channel region and these side channels will increase the effective channel width. In addition, slicing layout structure can suppress the self-heating effect and enhance the passivation efficiency. As a result, transistor slicing layout can obtain the higher current density compared with conventional layout method. By experimental results, the non-uniformity can be reduced 20% off. It is verified that the slicing layout in the driving

TFT not only can enhance the brightness in the panel but also can improve the non-uniformity problem.

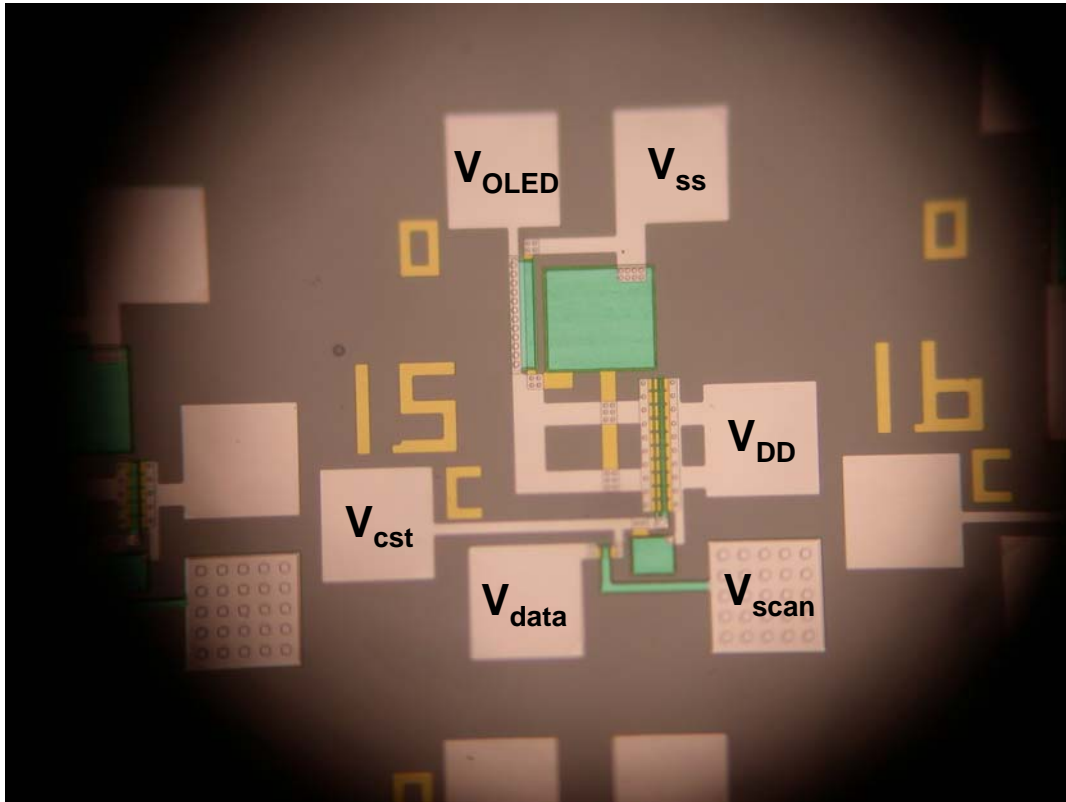


Fig. 3.12. Optical micrograph of conventional 2T1C pixel circuit.

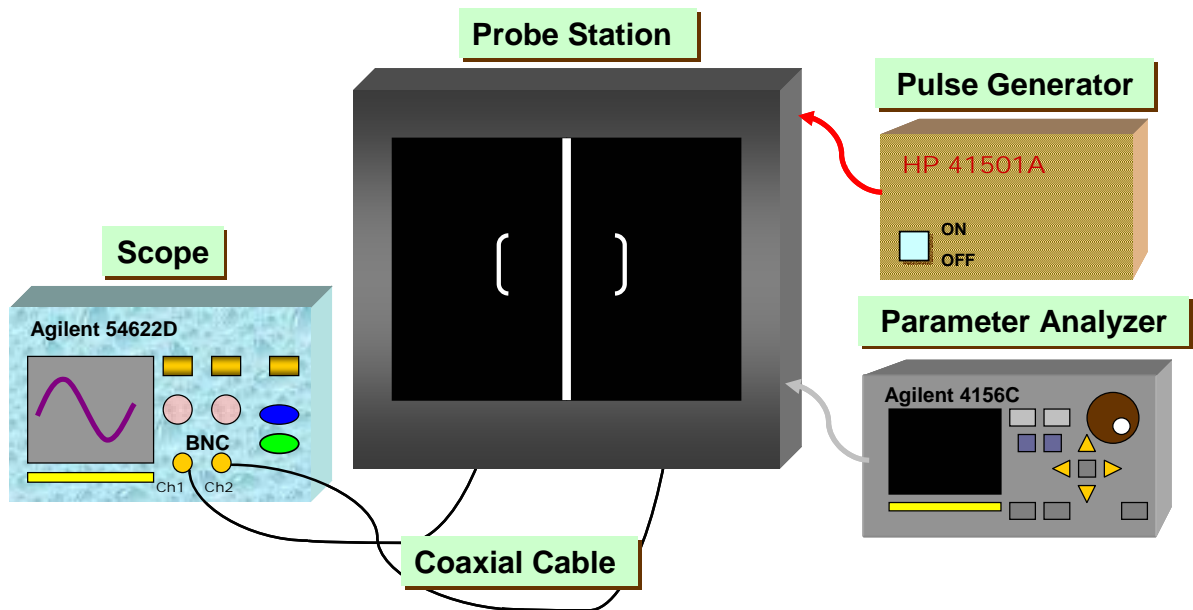


Fig. 3.13. Measurement system for conventional 2T1C testing pixels.

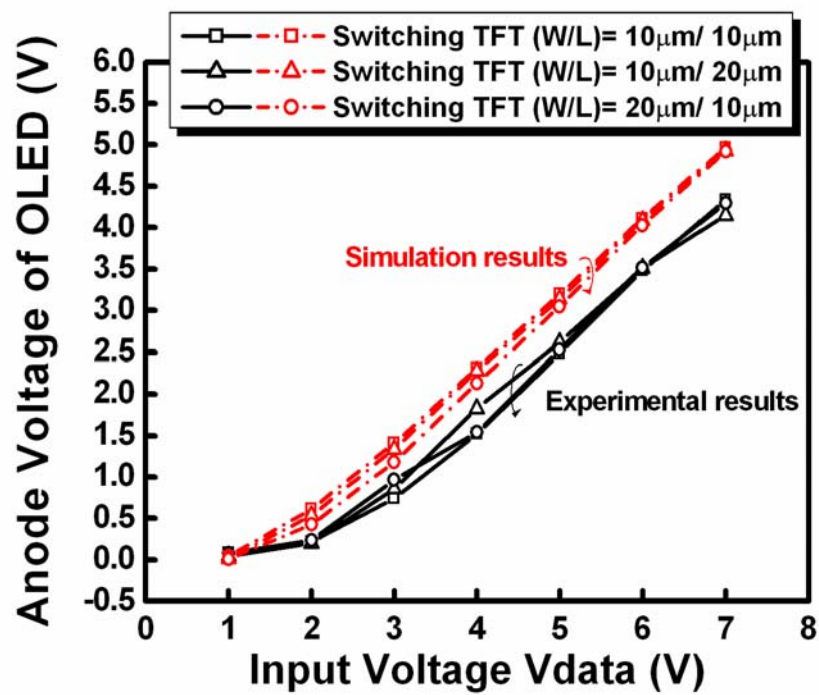


Fig. 3.14. The measured and simulation results of OLED anode voltages versus input voltages when the dimension of switching TFT varies.

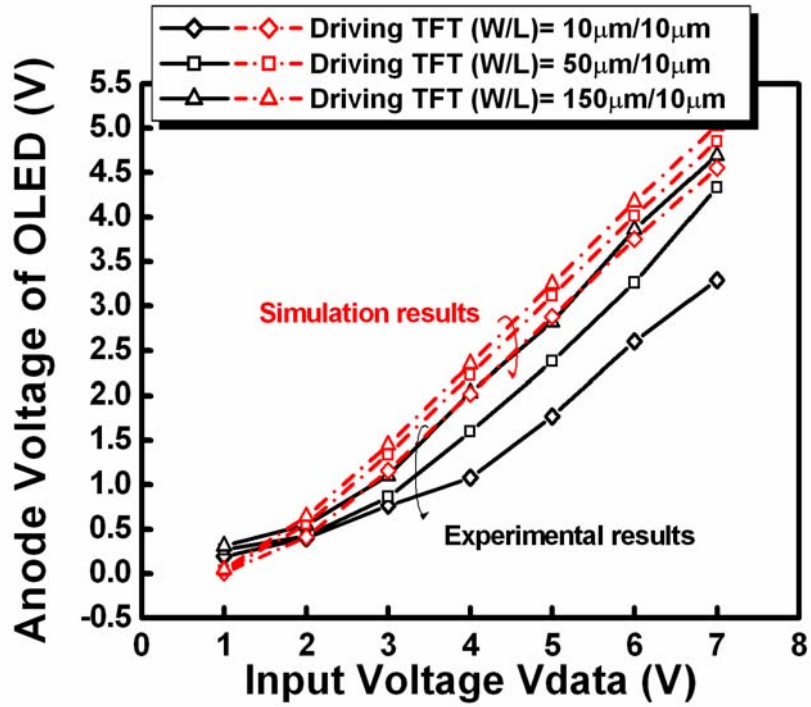


Fig. 3.15. The measured and simulation results of OLED anode voltages versus input voltages when the dimension of driving TFT varies.

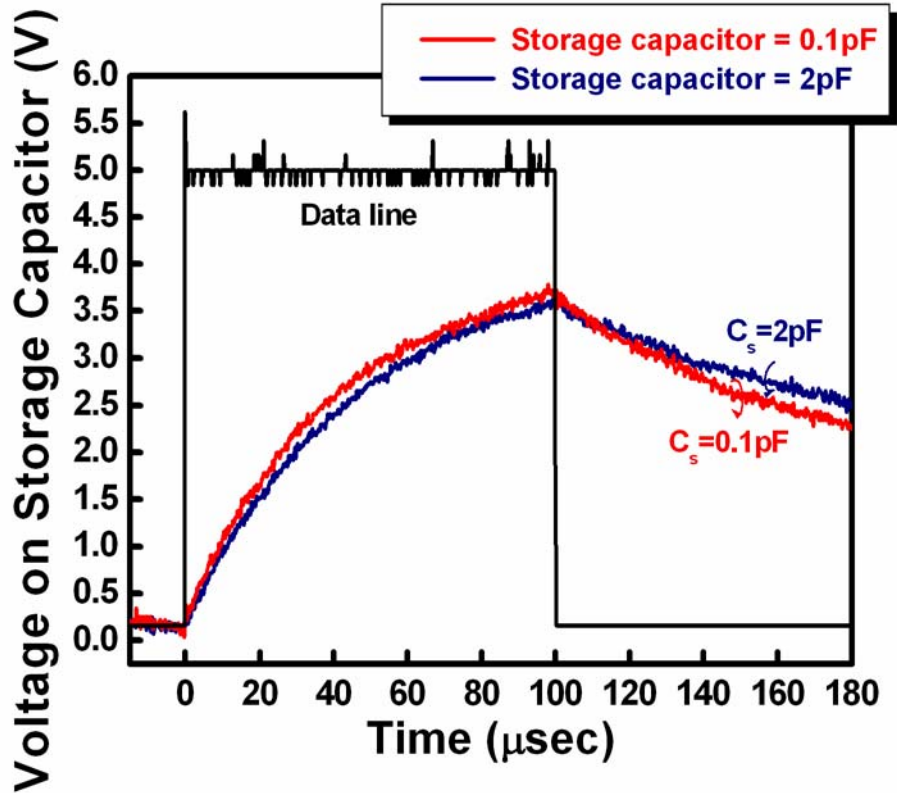


Fig. 3.16. The measured results of the stored voltage in the capacitor when $V_{data} = 5\text{V}$.

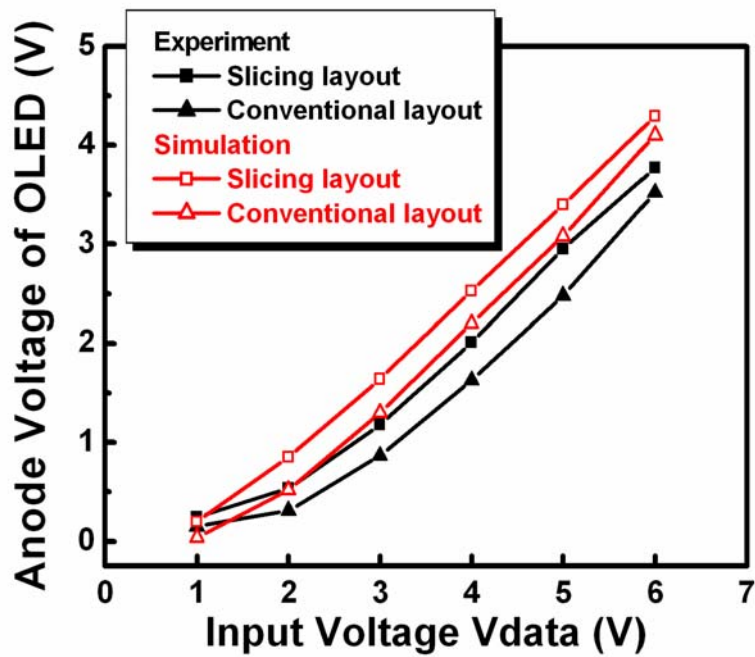


Fig. 3.17. The measured and simulation results of OLED anode voltages versus different input voltages.

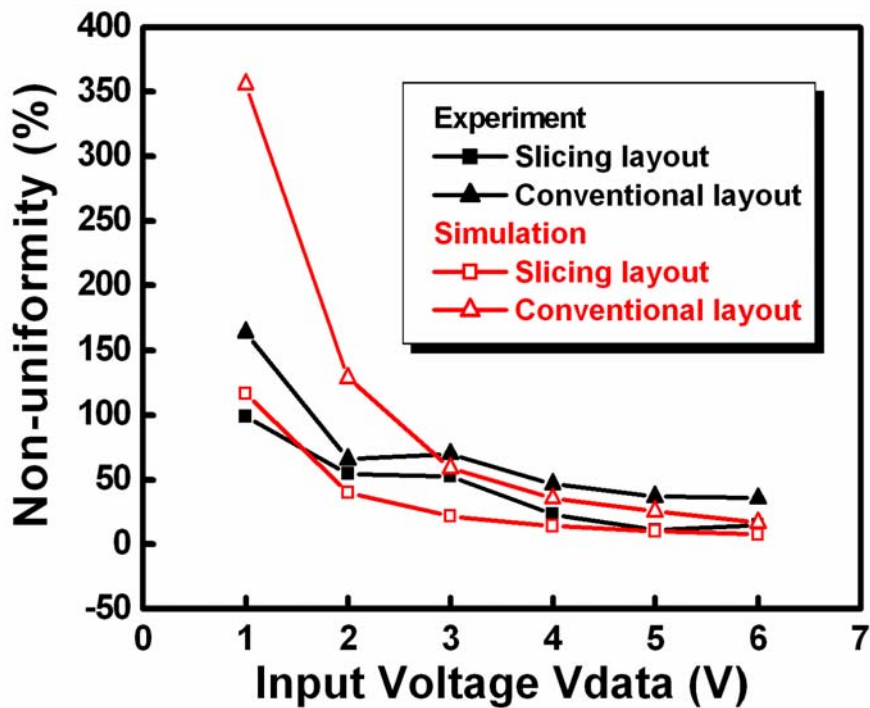


Fig. 3.18. The measured and simulation results of non-uniformity with conventional layout

and slicing layout.

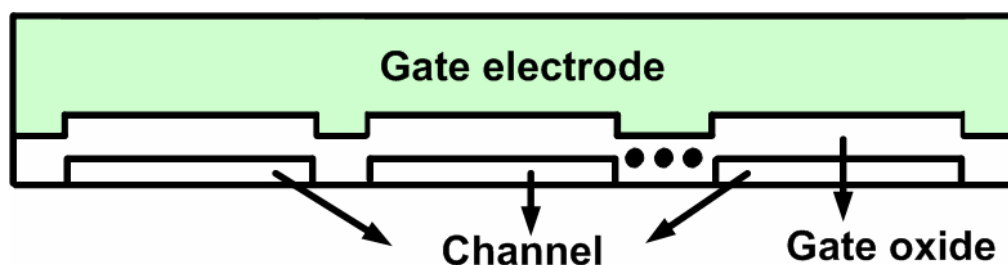


Fig. 3.19. Cross-section of driving TFT with slicing layout.

3.5 Summary

Conventional pixel circuits with two transistors and one capacitor (2T1C) have been investigated in detail in this chapter. By means of the results of simulation and experiment on the simple circuit design, the dimensional effects of transistors and storage capacitor on the circuit have been studied. In the traditional 2T1C circuit design, switching TFT is employed only as a switch element, so the dimension of the switching TFT is not an important factor in the circuit and can be reduced to the minimum value. Driving TFT plays a main role which is a constant current source to drive the OLED device. The larger of the driving TFT size, the larger of OLED anode voltage but the more area driving TFT occupies. The function of storage capacitor is to store the necessary gate voltage of driving TFT during the whole frame period. Although larger capacitor can hold the data voltage effectively, the charging time and the aperture ratio of the display will decrease consequently.

In addition to the basic component influence on the circuit, the effect of slicing layout of circuit is also investigated by simulation and experimental results. Due to the transistor slicing of driving TFT, the driving capability is enhanced to obtain brighter image for

display and the anode voltage of OLED can be raised above 30% at $V_{data}=3V$ by experimental results. It is attributed to the suppressing of the self-heating effect, increase of effective side channel width and enhancing the passivation efficiency. Therefore, the non-uniformity problem introduced during the fabrication process can be reduced effectively and the non-uniformity can be reduced 20% off.

